Voltammetric studies of aromatic nitro compounds: pH-dependence on decay of the nitro radical anion in mixed media

J. Carbajo [b], S. Bollo [a], L.J. Núñez-Vergara [a], P. Navarrete [a], J.A. Squella [a,*]

[a] *Bioelectrochemistry Laboratory, Chemical and Pharmaceutical Sciences Faculty, University of Chile, P.O. Box 233, Santiago 1, Chile*
[b] *Departamento de Química Física y Química Orgánica, Escuela Politécnica Superior, Universidad de Huelva, Huelva, Spain*

Abstract

In this report we have chosen ethyl-*m*-nitrobenzoate (EMNB) as a prototype of a nitroaromatic compound in order to carry out a detailed cyclic voltammetric study focused on the coupled chemical reaction of the generated nitro radical anion. The study was carried out in mixed media (water + DMF) at different DMF contents and several pH values on both mercury and carbon electrodes. In order to study the coupled chemical reaction it was necessary to choose a narrow pH range between 8 and 10. The coupled chemical reaction follows second order kinetics and we have used Olmstead's procedure to calculate the second order rate constant k_2. The k_2 values are strongly pH dependent. Typical values of $k_2 =$ are 1.68×10^4 l mol^{-1} s^{-1} and 1.15×10^4 l mol^{-1} s^{-1} for 60% DMF, pH 9.5 on mercury and GCE, respectively. Considering an EMNB concentration of 0.1 mM the corresponding half life time values were 0.59 s and 0.86 s.

Keywords: Nitroaromatics; Nitro radical anion; Cyclic voltammetry

1. Introduction

Electrochemical studies of aromatic nitro compounds have a long history in the chemical literature, having been discussed since the beginning of the twentieth century [1], but there is still a great interest in these types of molecule. One reason for such interest is that numerous nitro compounds are manufactured for use in pharmaceutical products and consequently they are introduced into living organisms where they are often involved in oxidation–reduction processes. The main pharmaceutical uses of nitroaromatic compounds are as antibacterial, antiprotozoal and anticancer agents [2–4]. The metabolic pathway of nitroaromatic compounds generates the radical anion in a one-electron reduction reaction [5]. This species exhibits cytotoxicity in several cellular systems, including mammalian, protozoan and bacterial cells [6–8]. Because of this, the nitro radical anion, a free radical species, has great significance in biological metabolisms.

Electrochemical techniques, especially cyclic voltammetry, have proved to be an important tool to study this radical species from different nitro compounds [9,10]. It is now well understood that a transfer of one electron initiates reduction of nitrobenzenes. The resulting radical anion is protonated and further reduced. Kastening and coworkers [11–16] showed that addition of surfactants results in a decrease in the rate of protonation that occurs at the electrode surface. The radical anion is then reduced at more negative potentials. Other authors have shown that a similar decrease in the rate of protonation occurs in the presence of aprotic solvent, such as 30–60% DMF [9,10,17,18]. More recently, Karakus and Zuman [19] have shown how the pH range in which a decrease in the rate occurs depends on the structure of the nitrobenzene and DMF concentration. Kastening [20,21], using electrogeneration of the nitro radical anion and following the homogeneous kinetics of its reaction using ESR and UV spectra, has shown that the nitro radical anion under-

E-mail address: asquella@ll.ciq.uchile.cl (J.A. Squella).

goes two competitive reactions, one of which is pH dependent and first order in the nitro radical anion, and the other is pH independent and second order in the nitro radical anion. In previous work we have found a second order chemical reaction for the nitro radical anion of several nitroaromatic drugs [22–25] and the corresponding second order rate constant (k_2) was calculated with the working curve described by Nicholson [26,27]. Furthermore, several authors [28–34] have studied the nitro radical anion interaction with amino thiols (e.g. glutathione), finding that these molecules interact with the nitro radical anion.

In this paper we have chosen ethyl-*m*-nitrobenzoate as a prototype of a nitroaromatic compound in order to carry out a detailed cyclic voltammetric study of the coupled chemical reaction of the generated nitro radical anion. This study was focused on mixed media (water + DMF) at different DMF contents and several pH values on both mercury and carbon electrodes. Specifically, we are interested in investigating the proton influence on the rate constant of the coupled chemical reaction, in order to study the relation between k_2 and pH. In order to investigate the influence of the electrode material in the chemical reaction of the nitro radical anion we have studied the reaction on both mercury and glassy carbon electrodes. Furthermore, we have also studied the interaction between the nitro radical anion and glutathione at different pH values on both mercury and carbon electrodes.

2. Experimental

2.1. Reagents and solutions

The ethyl-*m*-nitrobenzoate (EMNB) was prepared from *m*-nitrobenzoic acid, which is a commercial product, according to a well known esterification technique [35]. All the other reagents employed were of analytical grade.

Solutions for cyclic voltammetry were prepared by weighing an adequate quantity of EMNB in order to obtain a final concentration of 1 mM.

Experiments were made in mixed DMF + aqueous solutions (60:40 or 40:60). The aqueous solution was 0.015 M sodium citrate, 0.05 M boric acid and the ionic strength was kept constant with 0.3 M KCl and 0.1 M tetrabutylammonium iodide (TBAI). pH buffers between pH 8 and pH 10 were obtained by addition of NaOH or HCl to the sodium citrate + boric acid mixture used. All the working solutions were well buffered.

2.2. Apparatus

Voltammetric curves were recorded on a Autolab (Ecochemie model PGSTAT 20) instrument attached to a PC computer with proper software (GPES) for total control of the experiments and data acquisition and treatment.

All pH measurements were carried out with a Crison model Basic 20 (Resolution 0.01, precision ± 0.01) pH meter. The glass electrode was a Crison 52-02 and the standard solutions used for calibration were Crison 4.00 and 7.02 and Probus 10.00.

All experiments were carried out at a constant temperature of 25 ± 0.1°C using a thermostated Metrohm cell and the solutions were purged with pure nitrogen for 10 min prior to the voltammetric runs.

A static mercury drop electrode (SMDE) (Metrohm VA 663) with a drop area of 0.42 mm^2 was used as a working electrode and a platinum wire as a counter electrode. All potentials were measured against Ag | AgCl | KCl (3M). Also, a glassy carbon disk electrode (GCE) with an area of 2 mm^2 was used as the working electrode.

2.3. Methods

pH measurements were corrected according to the following equation [36]: $pH^* - B = \log U°H$; where pH* is equal to $-\log aH$ in the mixed solvent, B is the pH meter reading and the term $\log U°H$ is the correction factor for the glass electrode, which was calculated from the different mixtures of DMF and aqueous solvent, according to a previously reported procedure [37].

The return-to-forward peak current ratio I_{pa}/I_{pc}, for the reversible first electron transfer (the $Ar–NO_2/Ar–NO_2^{\bullet -}$couple) was measured for each cyclic voltammogram, varying the scan rate from 0.4 V s^{-1} up to 2.0 V s^{-1} according to the procedure described by Nicholson [26].

Using the theoretical approach of Olmstead et al. [27], the I_{pa}/I_{pc} values measured experimentally at each scan rate were inserted into a working curve to determine the parameter ω, which incorporates the effects of rate constant, drug concentration and scan rate. A plot of ω versus τ resulted in a linear relationship described by the equation

$$\omega = k_2 c_0 \tau$$

where k_2 is the second order rate constant for the decomposition of $ArNO_2^{\bullet -}$, c_0 is the nitro compound concentration and $\tau = (E_\lambda - E_{1/2})/v$. Consequently we can obtain the second order rate constant for the decomposition of the nitro radical anion from the slope of the straight line ω versus τ. The assumption that the decomposition of $ArNO_2^{\bullet -}$ follows second order kinetics is supported by the linear relation between the kinetic parameter ω and the time constant τ.

Furthermore, following the procedure described above to obtain k_2, it is possible to determine the pseudo-second-order constant k_{app}, in the presence of

glutathione. Then we can obtain the rate constant k_i for the interaction between the nitro radical anion and glutathione as follows. Considering the presence of glutathione the radical has two possible modes of decay, a natural decay and by interaction with glutathione,

$$2ArNO_2^{\bullet -} + 2H^+ \xrightarrow{k_2} ArNO_2 + ArNO + H_2O$$

$$ArNO_2^{\bullet -} + GSH \xrightarrow{k_i} \text{products}$$

The depletion of the radical has the following expression:

$$-\mathrm{d}[ArNO_2^{\bullet -}]/\mathrm{d}t$$

$$= 2k_2[ArNO_2^{\bullet -}]^2 + k_i[GSH][ArNO_2^{\bullet -}]$$

The apparent second order rate constant k_{app} is given by

$$k_{app} = 2k_2 + k_i[GSH]/[ArNO_2^{\bullet -}]$$

In the absence of glutathione $k_{app} = k_2$:

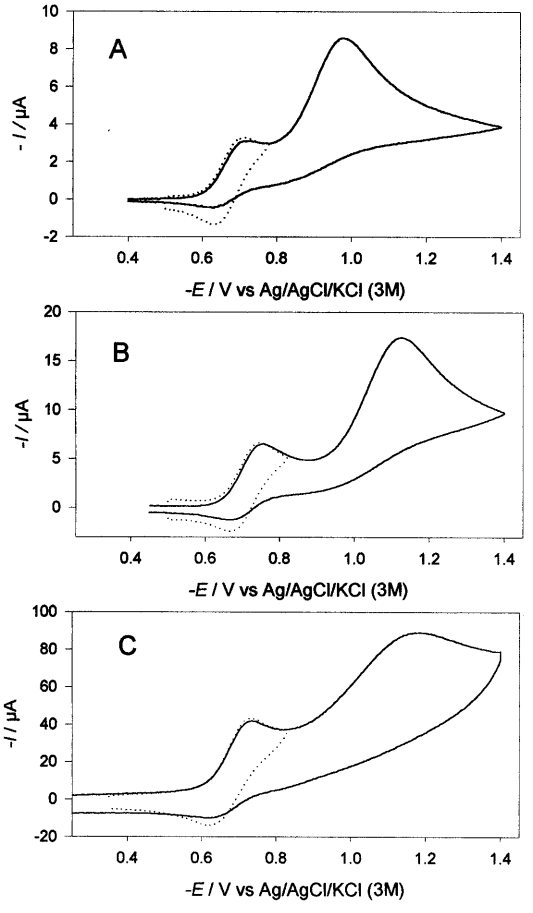

Fig. 1. Cyclic voltammograms of 1×10^{-3} M of EMNB in mixed media at different aquo/organic ratios on Hg and GC electrodes. (A) 40:60 DMF + aqueous buffer pH 9.6 on Hg. (B) 60:40 DMF + aqueous buffer pH 9.6 on Hg. (C) 40:60 DMF + aqueous buffer pH 9.6 on GCE. Sweep rate: 1 V s^{-1}. The dashed line shows a short sweep with the isolated first couple.

$$k_{app}/2k_2 = 1 + k_i[GSH]/2k_2[ArNO_2^{\bullet -}]$$

According to the last equation a plot of $k_{app}/2k_2$ versus the glutathione concentration should be a straight line with slope $k_i/2k_2[ArNO_2^{\bullet -}]$. Since k_2 is known and $[ArNO_2^{\bullet}]$ is assumed equal to $[ArNO_2]$, it is possible to obtain the rate constant for the interaction between glutathione and the nitro radical anion formed from EMNB.

3. Results and discussion

The cyclic voltammograms of EMNB in aqueous media at both HMDE and GCE show a single cathodic reduction peak corresponding to the four-electron reduction of the nitro group to form the corresponding hydroxylamine derivative as is usual for nitroaromatic compounds (data not shown). In mixed media the behaviour is rather different, but in this work we are concerned only with the behaviour in mixed media containing different percentages of DMF organic co-solvent (40–60%) with different electrode materials (Hg and GCE). In this media, at approximately pH > 7, the height of the four-electron peak in the presence of the organic co-solvent gradually decreases with increasing pH until it reaches the height corresponding to a one-electron reversible process. Simultaneously, at more negative potentials, an irreversible three-electron reduction wave is observed. In Fig. 1A we can observe the above described behaviour in the case of a cyclic voltammogram of 1×10^{-3} M EMNB in a mixed medium (40:60, DMF + aqueous buffer pH 9.6) on a mercury electrode. From this voltammogram we can distinguish a first reversible couple (I) due to the one-electron reduction of the nitro group to form the corresponding nitro radical anion and a second irreversible reduction peak (II) due to the subsequent reduction of the nitro radical anion according to the following equations:

$$ArNO_2 + e^- \rightleftarrows ArNO_2^{\bullet -} \quad (1)$$

$$ArNO_2^{\bullet -} + 3e^- + 4H^+ \rightarrow ArNHOH + H_2O \quad (2)$$

This behaviour was also observed on changing the DMF percentage to 60% (Fig. 1B) and the electrode material to glassy carbon (Fig. 1C). From these experiments we can appreciate that, in the case of the mercury electrode, the use of a higher DMF percentage produces a shift of the three-electron peak to more negative potentials. Consequently the separation between the one-electron peak and the three-electron peak was increased to about 100 mV when compared with the 40% DMF result. Considering that the three-electron step involves a first protonation of the radical anion with further reduction, the shifting of the peak to more negative potentials can be ascribed to hindrance

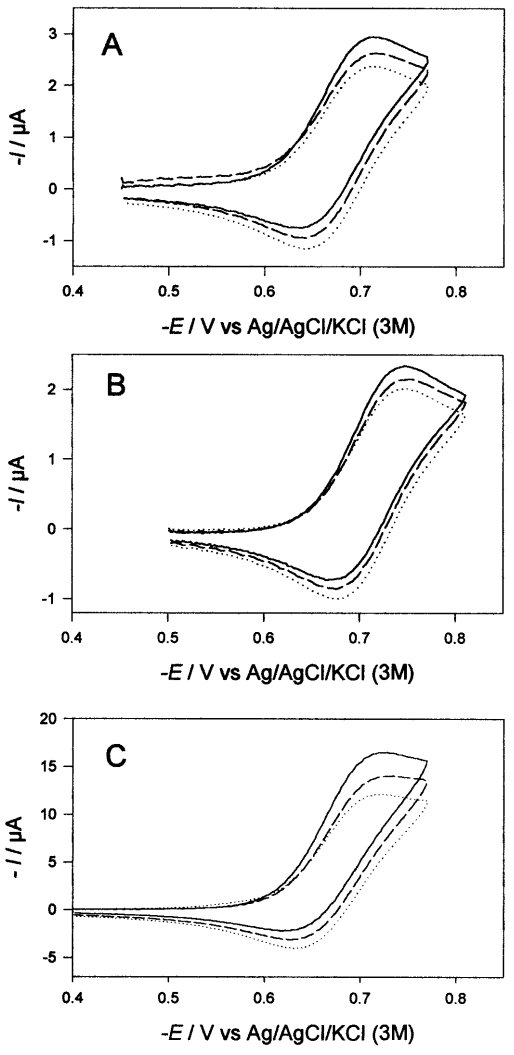

Fig. 2. Cyclic voltammograms showing the first reversible couple due to the one-electron reduction of EMNB at different pH values. (A) 40:60 DMF + aqueous buffer on Hg. (B) 60:40 DMF + aqueous buffer on Hg. (C) 40:60 DMF + aqueous buffer on GCE. (——) pH 8.4, (– – –) pH 9.4, (· · ·) pH 9.9.

of the protonation due to the difference in the organic co-solvent content. This fact can be attributed to the radical anions being more stable in solution than when adsorbed on the electrode surface, with the result that radical anions displaced from the electrode surface by the organic co-solvent are no longer involved in protonation and charge transfer at the same potential as those adsorbed [38,39]. On the other hand, when we compared the cyclic voltammograms at the same percentage DMF but on different electrode surfaces (Fig. 1A and C) we can also observe a considerable shift of the peak II to more negative potentials. In this case the results suggest that competitive adsorption also plays a role, preventing surface protonation of the radical.

From these experiments (Fig. 1) we can also conclude that the first electron transfer to form the nitro radical anion remains practically unaltered when both the percentage DMF and the electrode surface are changed. In order to study the nitro radical anion stability we have studied in isolation the couple due to the first electron transfer. In Fig. 2 we can observe the isolated couple at different pH values. This pH effect was studied at different DMF percentages and on both mercury and glassy carbon electrodes. Under all conditions the pH effect was similar, i.e. the potential peaks remain practically pH independent and the current ratio, I_{pa}/I_{pc}, increases when the pH increases. In the graphs of Fig. 3 we show the results obtained when varying both the scan rate and the pH. From these results we can conclude that in all cases I_{pa}/I_{pc} increased when the pH increased. Also, results show that as the scan rate increased, I_{pa}/I_{pc} increased towards unity. This diagnostic criterion fulfils the requirements for an irreversible chemical reaction following a reversible charge-transfer step, i.e. EC_i process. To check the order of the following chemical reaction, the dependence of the I_{pa}/I_{pc} ratio on the concentration of EMNB was evaluated. As predicted by Olmstead et al. [27] for a second order reaction, the I_{pa}/I_{pc} ratio decreases parallel with the increasing concentration of the electroactive species. The second order constants were assessed from cyclic voltammograms for EMNB for each case, according to Olmstead's procedure [27]. Confirming the second order character of the following chemical reaction, plots of the kinetic parameter, ω, versus the time constant, τ, were linear for all pH and surface electrode conditions (Fig. 4). From the slope of these straight lines we can obtain the second order rate constants, k_2, for the decay of the nitro radical anions at different pH values. The second order rate constant was strongly pH dependent due to the proton influence in the quenching reaction of the radical anion. From the above results it is possible to affirm that the reactions producing the couple are:

$$ArNO_2 + e^- \rightleftarrows ArNO_2^{\bullet -}$$

$$2ArNO_2^{\bullet -} + 2H^+ \xrightarrow{k_2} ArNO_2 + ArNO + H_2O \qquad (3)$$

In Fig. 5, the dependence between k_2 and pH for different experiments with different electrode surface and DMF content are shown. In all cases the stability of the nitro radical anion was increased when the pH increased. This result is in accord with the above Eq. (3), i.e. when the proton concentration decreases the decay reaction is not favoured. Furthermore, from the results in Fig. 5 we can observe that at higher DMF content (or lower H_2O content) the decay was increased. This result also is in accord with the above Eq. (3), i.e. when the H_2O concentration is lower the decay reaction is favoured.

We had to adjust the pH in a rather narrow range (pH 8–10) for adequate study of the pH dependence of the decay of the radical anion. This range is very critical because for values lower than 8 the protonation

of the nitro radical anion is favoured and consequently the one-electron couple was not well isolated. On the other hand, at pH higher than 10 the protonation is totally hindered, consequently the above Eq. (3) did not occur. In Fig. 3A (pH 10.4) we can observe that the current ratio remains unaltered at all sweep rates, showing that the nitro radical anion was not protonated in this time schedule. The results obtained in 60% DMF were more reliable because the couple was known to be best resolved in this case. We can observe in Fig. 1A that at the switching potential there is some contribution of the further peak. This effect in the switching potential is considerably optimized in the case of 60% DMF content (Fig. 1B). Typical values of k_2 are 1.68×10^4 l mol^{-1} s^{-1} and 1.15×10^4 l mol^{-1} s^{-1} for 60% DMF, pH 9.5 on mercury and GCE, respectively. Considering an EMNB concentration of 0.1 mM, the corresponding half life time values were 0.59 s and 0.86 s, respectively.

The nitro radical anion is considered to be quite stable. Therefore, its reactions with other biomolecules deserve further study. We [23,28,29], as well as others [33,34], have studied the interaction of nitro radical anions with aminothiols. In this paper we have studied the interaction of the nitro radical anion from EMNB with glutathione (GSH) on both mercury and GCE. Fig. 6 shows typical cyclic voltammograms of EMNB on a mercury electrode as a consequence of adding GSH. An evident decrease in the I_{pa}/I_{pc} values can be seen as the GSH concentration is increased. An additional effect of GSH is the appearance of a signal due to the redox behaviour of GSH on a mercury electrode according to the well known following reaction [40]:

$$GSH + Hg \rightleftarrows GSHg + H^+ + e^- \quad (4)$$

To estimate quantitatively the interaction rate constant (k_i) for the reaction between the nitro radical anion generated from EMNB and GSH the same approach as previously described [10] was used, and the results are shown in Fig. 7. From the slope of this graph a k_i value of 2.88×10^4 M^{-1} s^{-1} was obtained. Furthermore we have studied the interaction between EMNB and GSH on the GCE. Surprisingly, the cyclic voltammograms remained unaltered after adding GSH and consequently the I_{pa}/I_{pc} values are the same with and without GSH (Fig. 8) at different pH values. This fact means that the mercury interface is totally necessary for the interaction between the nitro radical and GSH. At the potential at which the radical is formed, GSH exists newly formed in the surface of the electrode (Eq. (4)), facilitating the interaction. This fact did not occur in the GCE. In spite of these results there is evidence in the literature [34] that the nitro radical anion obtained from the drug oxamniquine interacts with GSH on a GCE.

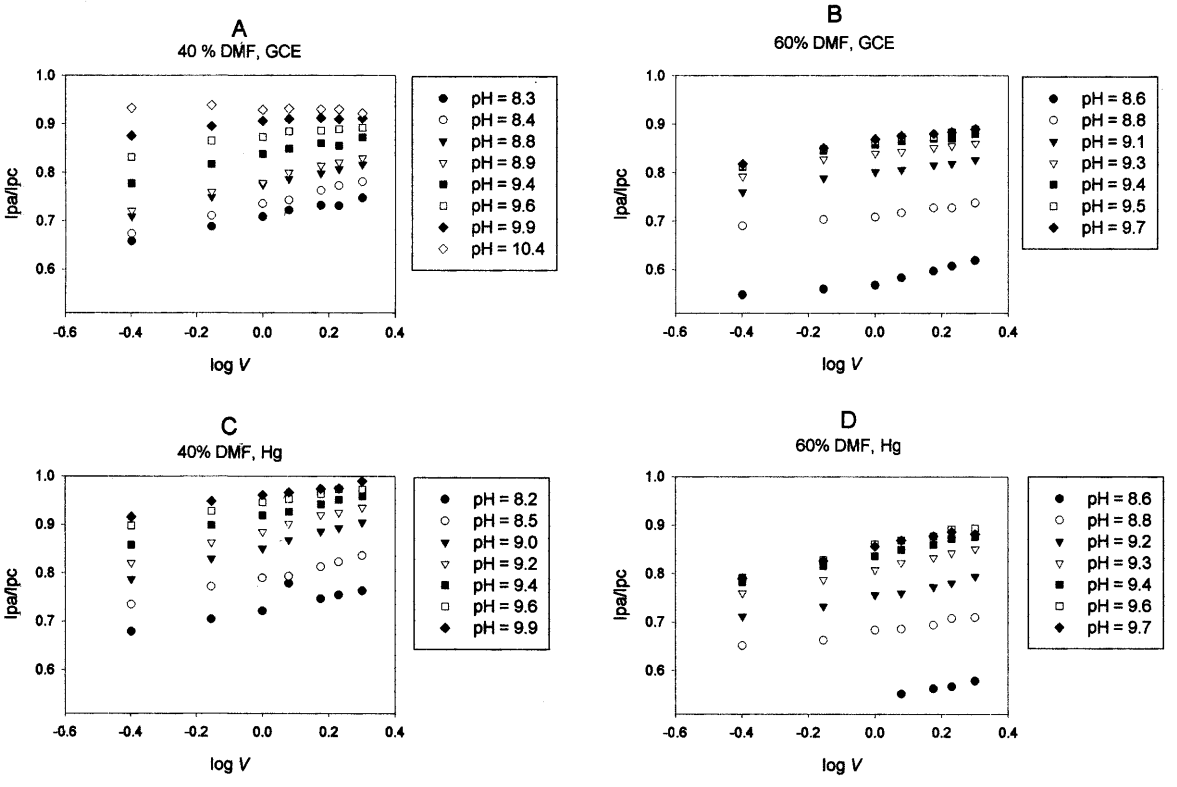

Fig. 3. Current ratio dependence on sweep rate at different pH values, DMF percentages and electrodes.

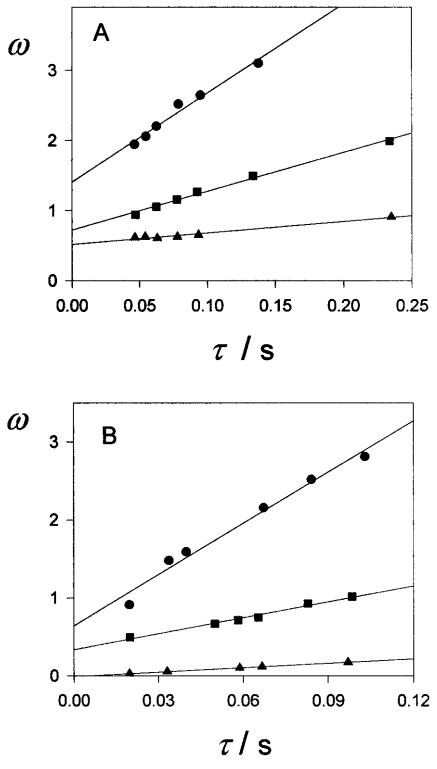

Fig. 4. Plot of the kinetic parameter, ω, with the time constant, τ, for EMNB at different pH values. (A) 40:60 DMF + aqueous buffer on GCE, (●) pH 8.4, (■) pH 9.4, (▲) pH 9.9. (B) 60:40 DMF + aqueous buffer on Hg, (●) pH 8.9, (■) pH 9.4, (▲) 10.2.

4. Conclusions

The results of experimental work presented above, as well as those of previous workers in this field, can be summarized in the following points.

The use of higher concentrations of DMF (60%) produces an optimal separation between the irreversible three-electron peak and the reversible couple due to the reduction of the nitro group to the nitro radical anion. Consequently, in order to obtain a pure reversible couple avoiding any contribution of faradaic current at the switching potential, 60% DMF is recommended.

The reversible mono-electronic couple remains unaltered when the DMF content and the electrode material are changed. From the pH dependence of the reversible couple, only a change in the current ratio, while the potential peaks remained unaltered, was observed. This fact implies that the pH change affects a coupled chemical reaction following the electron transfer.

The following coupled reaction fulfilled the requirements for a second order chemical reaction but in order to study this reaction the pH must be adjusted in a narrow range between 8 and 10. In this range the protonation of the nitro radical anion is sufficiently favoured and consequently the one-electron couple was not isolated. On the other hand, at pH values higher than this range the protonation is totally hindered and the second order chemical reaction does not occur. Inside this range the second order chemical reaction behaves according to the above Eq. (3), wherein protons favour the occurrence of the reaction and a high content of water hinders the reaction.

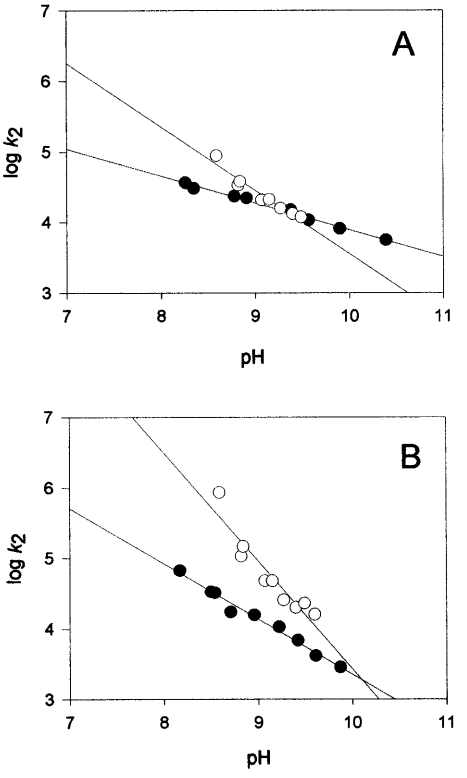

Fig. 5. pH dependence of the natural decay, k_2, of the nitro radical anion for different water contents and electrode materials. (A) Glassy carbon electrode and (B) mercury electrode. (●) 40% DMF, (○) 60% DMF.

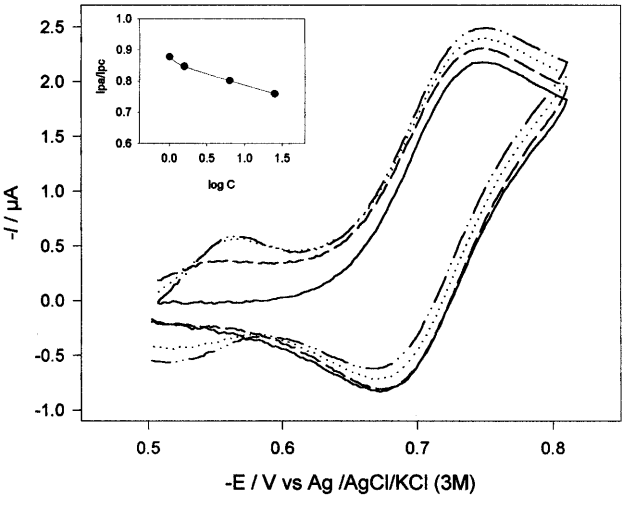

Fig. 6. Effect of adding GSH on the cyclic voltammogram of 1×10^{-3} M EMNB on a mercury electrode. Insert: current ratio dependence on GSH concentration. (——) 0 mM, (– – –) 0.2 mM, (· · ·) 0.8 mM, (—) 1.4 mM.

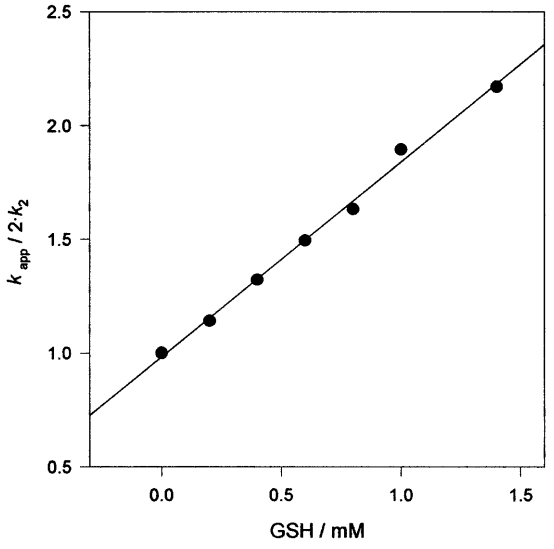

Fig. 7. Plot of $k_{app}/2k_2$ versus GSH concentration.

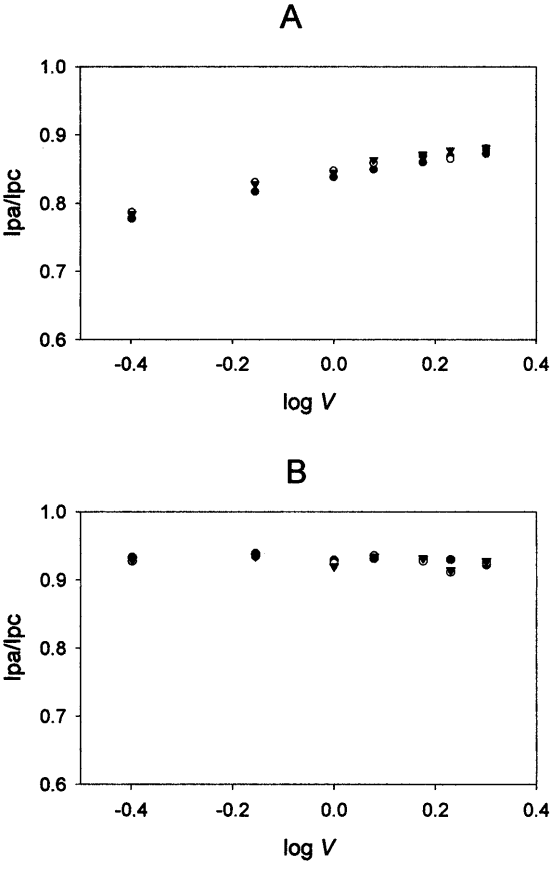

Fig. 8. Effect of adding GSH on the cyclic voltammogram of 1×10^{-3} M EMNB on GCE. Current ratio dependence with the sweep rate at different GSH concentrations. (A) pH 9.6, (B) pH 10.4. (●) 0 mM, (○) 1 mM, (▼) 2 mM.

The k_2 values obtained are practically the same when calculated for the reaction at the mercury or the glassy carbon electrode, however the interaction between GSH and the nitro radical anion was observed only on Hg.

Acknowledgements

This research was supported by grant 8000016 from FONDECYT. Also financial support from Junta de Andalucía, España for J. Carbajo is acknowledged.

References

[1] K. Brand, Die Elektrochemische Reduction Organisher Nitrokorper, Stuttgart, 1998.
[2] D. Greenwood, Antimicrobial Chemotherapy, Oxford University Press, 13th edn., 1995.
[3] L.P.H. Logan, P.A. Gummet, J.J. Misiewicz, Q.N. Karim, M.M. Walker, G.H. Baron, Lancet II (1991) 1449.
[4] G.E. Adams, Radiat. Res. 132 (1992) 129.
[5] J.E. Biaglow, B. Jarabson, C.L. Greenstuck, J. Raleigh, Mol. Pharmacol. 13 (1977) 269.
[6] J.E. Biaglow, M.E. Varnes, L. Roizer-Towle, E.P. Clark, E.R. Epp, M.B. Astor, E.J. Hall, Biochem. Pharmacol. 35 (1986) 77.
[7] J.R. Ames, V. Hollstein, A.R. Gagneux, M.D. Ryan, P. Kovacevic, Free Radical Biol. Med. 3 (1987) 85.
[8] J.R. Ames, M.D. Ryan, P. Kovacevic, Free Radical Biol. Med. 2 (1986) 277.
[9] L.J. Núñez-Vergara, S. Bollo, A. Alvarez, M. Blazquez, J.A. Squella, J. Electroanal. Chem. 345 (1993) 129.
[10] L.J. Núñez-Vergara, F. García, M. Dominguez, J. De la Fuente, J.A. Squella, J. Electroanal. Chem. 381 (1995) 215.
[11] L. Holleck, B. Kastening, Z. Elektrochem. 63 (1959) 177.
[12] B. Kastening, L. Holleck, Z. Elektrochem. 64 (1960) 823.
[13] L. Holleck, B. Kastening, R.D. Williams, Z. Elektrochem. 66 (1962) 396.
[14] B. Kastening, J. Electroanal. Chem. 24 (1970) 417.
[15] B. Kastening, L. Holleck, J. Electroanal. Chem. 27 (1970) 355.
[16] L. Holleck, B. Kastening, M. Vogt, Electrochim. Acta 8 (1965) 255.
[17] J.H. Tocher, D.I. Edwards, Free Radical Res. Commun. 4 (1988) 269.
[18] J.H. Tocher, D.I. Edwards, Free Radical Res. Commun. 16 (1992) 19.
[19] C. Karakus, P. Zuman, J. Electroanal. Chem. 396 (1995) 499–505.
[20] B. Kastening, Electrochim. Acta 9 (1962) 241.
[21] B. Kastening, Collect. Czech. Chem. Commun. 30 (1965) 4033.
[22] S. Bollo, L.J. Núñez-Vergara, J.A. Squella, Bol. Soc. Chil. Quím. 44 (1999) 67.
[23] L.J. Núñez-Vergara, M.E. Ortiz, S. Bollo, J.A. Squella, Chem. Biol. Interactions 106 (1997) 1.
[24] J.A. Squella, J. Mosre, M. Blazquez, L.J. Núñez-Vergara, J. Electroanal. Chem. 319 (1991) 177.
[25] A. Alvarez-Lueje, H. Pessoa, L.J. Núñez-Vergara, J.A. Squella, Bioelectrochem. Bioenerg. 46 (1998) 21.
[26] R.S. Nicholson, Anal. Chem. 36 (1964) 1406.
[27] M.L. Olmstead, R.G. Hamilton, R.S. Nicholson, Anal. Chem. 41 (1969) 260.
[28] J.A. Squella, S. Bollo, J. De la Fuente, L.J. Núñez-Vergara, Bioelectrochem. Bioenerg. 34 (1994) 13.
[29] L.J. Núñez-Vergara, F. García, M. Dominguez, J. De la Fuente, J.A. Squella, J. Electroanal. Chem. 381 (1995) 215.
[30] L.J. Núñez-Vergara, P. Navarrete, M.E. Ortiz, S. Bollo, J.A. Squella, Chem. Biol. Interactions 101 (1996) 89.
[31] L.J. Núñez-Vergara, G. Diaz-Araya, C. Olea-Azar, A.M. Atria, S. Bollo, J.A. Squella, Pharm. Res. 15 (1998) 1690.
[32] J.A. Squella, P. Gonzalez, S. Bollo, L.J. Núñez-Vergara, Pharm. Res. 16 (1999) 161.

[33] J.H. Tocher, D.I. Edwards, Biochem. Pharmacol. 48 (1994) 1089.
[34] A. Radi, F. Belal, J. Electroanal. Chem. 441 (1998) 39.
[35] A.I. Vogel, A Textbook of Practical Organic Chemistry, Longmans, New York, 3rd edn., 1964, p. 782.
[36] A.G. Gonzalez, F. Pablos, A. Asuero, Talanta 39 (1992) 91.
[37] A. Asuero, M.A. Herrador, G. Gonzalez, Talanta 40 (1993) 479.
[38] S.G. Mairanovskii, J.P. Stradins, I.Y. Kravis, Sov. Electrochem. 8 (1972) 766.
[39] J.M. López-Fonseca, M.C. Gomez Rivera, J.C. García Monteagudo, E. Uriarti, J. Electroanal. Chem. 347 (1993) 277.
[40] M. Stankovich, A. Bard, J. Electroanal. Chem. 75 (1977) 487.